Hydrogen trapping in ^{3}He-irradiated Fe

Ikuji Takagi*, Kotaro Matsuoka, Toshiyuki Tanaka, Masafumi Akiyoshi, Takayuki Sasaki

Graduate School of Engineering, Kyoto University

Kyoto Daigaku-Katsura, Kyoto 615-8540, Japan

ABSRACT

The characteristics of irradiation-induced hydrogen (deuterium) traps in pure Fe were investigated for quantitative evaluation of tritium retention in fusion reactor components. The deuterium depth profiles of an Fe disk sample exposed to deuterium plasma were observed by means of nuclear reaction analysis (NRA) before and after irradiation with 0.8 MeV or 1.3 MeV ^{3}He ions. Irradiation generated a number of traps, and deuterium retention was drastically increased subsequent to irradiation. Steady-state deuterium concentration in the trap and the solution sites were obtained by continuously charging the sample with deuterium during the NRA. Based on these values, the trapping energy, which is the enthalpy difference between the two sites, was estimated to be 0.38 eV. The number ratio of the trap to atomic displacement was 0.013. Some of the traps were annihilated around 523 K. The annihilation temperature, the trapping energy, and the equilibrium constant suggest that the trap is a dislocation loop introduced by the irradiation. It is deduced that the tritium inventory in the Fe components of a reactor should be drastically increased by neutron irradiation due to the formation of traps, but may be significantly reduced by high temperature operation of the components.

*Corresponding author; takagi@nucleng.kyoto-u.ac.jp

1. Introduction

Fe is a base element of candidate alloys for structural components of fusion reactors such as ferritic steel and stainless steel. Heavy fast-neutron irradiation of the components of the fusion reactor results in significant irradiation damage, and irradiation-induced defects are produced that may act as hydrogen traps to increase tritium retention. For quantitative evaluation of the tritium retention, the characteristics of the traps such as the trapping energy and the trap density must be known. There is, however, a dearth of available data delineating hydrogen trapping in irradiation-damaged Fe.

Hydrogen trapping in Fe is conventionally investigated using a time-lag method [1]. The apparent diffusion coefficient, D_e, is estimated from a lag time in the transient behavior of hydrogen permeation, and the trapping energy is derived from the temperature dependence of D_e [2-5]. This method, however, is not easily applied to an ion-irradiated sample where traps are produced in a very small part of the sample so that they would not affect the permeation behavior. Thermal desorption analysis (TDS) is another technique that is often used for ion-irradiated samples, but is also difficult to apply to Fe given that the heat of solution of hydrogen in Fe is positive and hydrogen is easily desorbed from Fe even at relatively low temperatures. In a modified TDS technique developed by Myers [6], the temporal evolution of the residual deuterium concentration is monitored using NRA and quantitatively analyzed by considering hydrogen diffusion and trapping; these empirical analyses have been conducted at non-steady state.

The present study utilizes an in situ observation technique [7] for characterization of the hydrogen trap. This is a new method in which the deuterium depth profiles of a sample are measured by means of NRA under continuous deuterium charging from a plasma source. Given that the deuterium concentrations at the steady-state can be evaluated from the experiment, the trapping energy and the trap density can be derived from the temperature dependence of the concentrations.

2. Experimental

A disk-shape sample specimen of iron with a diameter of 48 mm and a thickness of 2.0 mm was cut from a plate, which was hot-rolled at 1473 K by Daido Steel Co. Ltd. The sample purity was 99.99 % and main impurities were C: -10, S: -10, O: -360, N: -40, Si: <20, and P: <20 ppm by weight. Prior to the experiment, the transient behavior of deuterium plasma-driven permeation [8] through the sample was measured and the apparent diffusion coefficient of deuterium, D_e, was determined by the time-lag method. Between 350 and 600 K, D_e is expressed as:

$$D_e = 3.04\times10^{-8}\exp(-0.065[\mathrm{eV}]/kT) \qquad \mathrm{m^2s^{-1}} \qquad (1)$$

Here, k is the Boltzmann constant and T is the sample temperature. The determined activation energy of 0.065 eV is consistent with the literature data of 0.069 eV [9], which indicates that there are no intrinsic traps in the sample; thus, D_e in Eq. (1) is taken as the deuterium diffusion coefficient, D.

Details of the in situ observation technique have been provided elsewhere [10] and will be briefly described here. A sample was set between two vacuum chambers and one side of the sample was exposed to deuterium RF plasma. The RF power was 20 W and the discharge pressure was 1 Pa. The typical energy of deuterium particles incident to the sample was 1 eV [11], which was too small to produce radiation defects or cause a temperature change. Deuterium permeation flux through the sample was observed using a quadrupole mass analyzer. After the permeation reached the steady-state, the plasma-exposed side of the sample was irradiated with ^{3}He ions at an angle of 45º from the 4 MV van de Graaff accelerator of Kyoto University.

Before and after irradiation, deuterium depth profiles near the surface were measured by means of NRA using the reaction of D(^{3}He,p)^{4}He. A ^{3}He$^+$ beam was injected from the same accelerator and the proton energy spectrum was converted [12] to a deuterium depth profile from the surface to 1.5 μm -depth. The ion beam flux was kept below 1×10^{16} m^{-2}s^{-1} to prevent an increase in the sample temperature. The ion beam fluence at each NRA was limited to 2 $\times10^{19}$ m^{-2} to minimize irradiation effects. It should be noted that the sample was continuously

exposed to the plasma during the irradiation and the NRA so that the deuterium concentration was observed under steady-state permeation. The experimental conditions used for the four samples are summarized in Table 1, where Q is the number of displacement per atom averaged over the damage region.

3. Results

3.1 Deuterium depth profiles

Fig. 1 shows the deuterium depth profiles for sample A at 453 K before and after irradiation. Prior to irradiation, no deuterium was observed in the bulk. A small peak, attributed to deuterium absorption on the surface, was present at 0-depth. Due to the finite resolution of the NRA system, deuterium appears to be present at negative depth. Considering the depth resolution of 0.15 μm at FHWM and the probe depth, the region between 0.2 and 1.4 μm depth is hereafter regarded as bulk. It is known from the time-lag measurement that the diffusion is the rate-determining process of permeation in the present experiment. In the diffusion-limited permeation, the deuterium concentration in a solution site, C_s, is expressed by:

$$J = DC_s / L \qquad (2)$$

where L is the sample thickness. Given that J was 1.0×10^{18} $m^{-2}s^{-1}$ at 453 K, C_s was estimated to be 3.4×10^{23} m^{-3}, which was much lower than the detection limit of the NRA system of 2×10^{25} m^{-3}. It is reasonable that no significant observation of deuterium in the bulk was apparent from the NRA. A concentration gradient of deuterium in the solution site from the front to the back surfaces should be present. Nevertheless, the C_s in the NRA region is taken as constant because the sample thickness is much larger than the probe depth of the NRA.

Subsequent to irradiation of sample A with ^{3}He ions, the deuterium concentration in the bulk increased and a peak appeared at 0.9 μm depth, as shown in Fig. 1. The average deuterium concentration subsequent to irradiation was 7.8×10^{26} m^{-3}, which was more than 2000 times larger than the C_s, indicative of the production of numerous traps by the irradiation.

The depth profile of trapped deuterium in sample A is shown in Fig. 2. There is a concentration difference in the two profiles acquired before and after irradiation. The distribution of vacancies and ^{3}He ions estimated from the TRIM code [13] are also shown in arbitrary units. The figure shows that the peak depth in the profile is the same as that in the vacancy distribution but is smaller than the ion distribution. The region in which deuterium is present simply corresponds to the region of vacancy production, while no ^{3}He ions are present below 0.5 -μm depth. It is clear that the trap is not associated with ^{3}He ions but with radiation damage.

Fig. 3 shows the depth profile of trapped deuterium in sample D, irradiated at a higher energy than sample A. Again, the profile is very similar to the vacancy distribution. The FWHM of the peak in the profile is 0.41 μm when the depth resolution of the detection system is taken into account; this is nearly the same as that of 0.38 μm in the vacancy distribution. This agreement is also seen in the case of sample A shown in Fig. 2, which suggests negligible migration of the trap during or after irradiation.

3.2 Trapping energy

The trapping energy is defined here as the enthalpy difference between the solution and the trap sites. In the diffusion-limited permeation, there should be quasi-equilibrium of hydrogen between the two sites, and the equilibrium constant, *f*, is expressed [14] as

$$f = C_s(C_0 - C_t)/hNC_t \qquad (3)$$

where C_0 and hN are the density of the trap and the solution sites, respectively, and C_t is the concentration of hydrogen in the trap site; h is the number of solution sites per host atom, and N is the density of the host atom. In Fe, hydrogen is dissolved in an octahedral site [15], and h is taken as 3 [16]. Eq. (3) can be derived by analogy with the law of mass action; hence, f is related to the trapping energy, E_t, according to the following relation:

$$f = f_0 \exp(-E_t/kT) \qquad (4)$$

where f_0 is the pre-exponential factor representing the entropy difference between the two sites.

C_t can be directly observed using NRA, and C_s can be estimated from Eq. (2) using the steady-state permeation flux, J. The temperature dependence of C_t and C_s for sample A is shown in Fig. 4. The value of C_s increases with the sample temperature, whereas C_t increases with decreasing sample temperature to reach a saturation value of 1.25×10^{27} m^{-3}. The saturation value is taken as the trap density, C_0, given that all of the trap sites should be occupied by deuterium at saturation. Here, all of the parameters on the right side of Eq. (3) are given and f is determined for samples A and B as shown in Fig. 5. The reproducibility of f for the two samples is good, and f can be expressed by one equation:

$$f = 0.024 \exp(-0.38[\text{eV}]/kT) \quad (5)$$

The good linearity of the data indicates that the trap is a single species with a trapping energy of 0.38 eV. This trapping energy is higher than the value of 0.28 eV for ion-irradiated stainless steel [17] and that of 0.24 eV for nickel [10].

3.3 Trap production

Because the trap is associated with irradiation damage, its production can be related to atomic displacement. The evolution of the trap density, C_0, with displacement (for all of the samples) is shown in Fig. 6. Here, the number of displacements is estimated from the TRIM code [13] by assuming that the displacement energy is 25 eV and one vacancy corresponds to one displacement. C_0 is observed to increase almost linearly with displacement, and no tendency towards saturation is observed. This is probably because a fraction of the trap density, C_0/hN, is much less than unity, i.e., 0.0074 at maximum. In the case of low C_0/hN, a lot of normal sites persist so that the trap does not experience interference from other traps or with a collision cascade arising from the irradiation. Assuming that the number of traps is proportional to the displacement, the corresponding proportionality constant, referred as the trap production ratio herein, is estimated to be 0.013.

The trap production ratio should be much smaller than unity, considering the very low probability of survival of the radiation defects subsequent to short-time annealing just after the collision cascade. A detailed consideration is, however, difficult given that estimation of the production ratio depends on the displacement energy, which has not been accurately determined. Notably, the trap production ratio obtained in the present study is a moderate value compared with those of other metals such as 0.015 for Ni [18], 0.021 for V [19] and 0.007 for Mo [20].

4. Discussion

In previous empirical evaluations of the microstructural changes of Fe and steels induced by irradiation with energetic particles, dislocation loops have been most commonly observed [21-24]. Dislocation loops are considered to be interstitial type [21, 22]. Voids or bubbles have also been observed [21], but these tended to be produced at higher fluences. In the case of hydrogen irradiated steel [24], the number density of the dislocation loops begins to decrease at 523 K. In the case of neutron irradiated steel [23], the number density of the dislocation loops at 673 K is much less than that at 523 K. It is known that hydrogen is trapped by a dislocation in deformed Fe and steel. The trapping energy in the dislocation ranges from 0.28 eV [4, 25, 26], through 0.47 eV [27] to 0.62 eV [3]. Large scattering in these data may be attributed to a reduction of cold work. For example, the trapping energy is 0.28 eV for 9% reduction [4] and 0.62 eV for 60% reduction [3].

Fig. 4 shows that the deuterium concentration decreased to 40% after annealing the sample at 568 K for 1 h, whereas the permeation flux, that is, the deuterium concentration in the solution site remained unchanged. In the case of sample B, the deuterium concentration decreased to 30% when the sample temperature was maintained at 523 K for 20 h. This decline occurs because some of the traps were annihilated by the annealing process. Eq. (5) shows that the value of f_0 (0.024) deviates significantly from unity, which suggests that the trap is not a point defect given that a small entropy difference between the solution site and a point defect is expected, and hence f_0 should be close to unity. The trapping energy of 0.38 eV

lies within the range of the forementioned literature data. These results indicate that the trap observed in the present work is a dislocation loop produced by ^{3}He irradiation. Other types of the traps, including grain boundaries [27], single vacancy [6], vacancy clusters [6] and microvoids [26], are less plausible. Grain boundaries are present prior to the irradiation, but no traps are observed by NRA. A single vacancy would be annihilated by annealing in the present temperature range, or stabilized by forming of helium-vacancy complexes [28]. The trapping energy in vacancy clusters is much higher than 0.38 eV [6]. Microvoids would not be so different from vacancy clusters.

Because the hydrogen concentration in the solution site, C_s, is affected by the incident hydrogen flux, surface recombination, and diffusion, C_s may vary over a wide range in the fusion components. The dependence of the trap site occupancy, C_t/C_0, and the concentration ratio, C_t/C_s, on the solution site occupancy, C_s/hN, estimated from Eq. (3) is shown in Fig. 7. The equilibrium constant, f, is set to fixed values of 10^{-7}, 10^{-6}, and 10^{-5}, which correspond to 356 K, 437 K, and 566 K, respectively. Under the conditions given for Fig. 7, C_t/C_s is much higher than unity, and the total hydrogen concentration is almost equal to C_t. C_t/C_0 increases linearly with C_s/hN until C_s/hN becomes comparable to f, that is, f is an indicator of C_s/hN whether C_t/C_0 becomes saturated or not. The tritium inventory can be effectively reduced by maintaining f at a high value by heating the fusion reactor component in order to achieve the condition: $C_s/hN < f$.

In the fusion reactor, the plasma-facing components are irradiated with fast neutrons whereas the samples in the present work were irradiated with ^{3}He ions. Dislocation loops are also produced in steel by neutron irradiation [23]. Even though the plasma-facing components are not irradiated with ^{3}He ions, the number of ^{3}He atoms in these components may increase due to radioactive decay of tritium. In this sense, irradiation with ^{3}He simulates the effects of neutron irradiation and tritium retention. Because helium is considered to effectively produce dislocation loops [21], it is possible that an increase of the ^{3}He concentration by decay of trapped tritium enhances trap production and multiplies the tritium inventory. Base on the result of the present work, however, the tritium inventory in components made of Fe can be

drastically decreased by temporary heating or by maintaining a high temperature, typically 600 K.

5. Summary

An in situ observation technique, in which a sample is continuously charged with deuterium along with depth profiling of deuterium, was applied to pure Fe irradiated with MeV ^{3}He ions. Quasi-equilibrium was achieved in the Fe-D system, and certain important parameters of the trap density, C_0, the equilibrium constant, f, and the trapping energy of 0.38 eV were successfully determined. From the perspective of safe operation of fusion reactors, evaluation of the upper limit of the tritium inventory in the reactor components is very important. Because C_0 is a simple indicator of the upper limit, the characteristics of trap production and annihilation are of great concern. It was found that the number of traps was directly related to the atomic displacement, i.e., the trap production ratio was 0.013, and the annihilation onset temperature was around 523 K.

Given that iron-based alloys are used as the structural materials of fusion reactor components in practice, the present study is a first step, and investigation of iron-based alloys is the subject of further studies.

Acknowledgement

This work is supported by a Grant-in-aid for Scientific Research for Priority Area 476, “Tritium Science and Technology for Fusion Reactor.”

References

[1] J. Crank, The Mathematics of Diffusion, Second ed., Clarendon, Oxford, 1975. p.44.

[2] H. Hagi, Y. Hayashi, and N. Ohtani, Trans. Jpn. Inst. Met., 20 (1979) 349.

[3] A.J. Kumnick, H.H. Johnson, Acta. Metall. 28 (1980) 33.

[4] H. Hagi, Y. Hayashi, Trans. Jpn. Inst. Met. 28 (1987) 368.

[5] E. Serra, A. Perujo, G. Banamati, J. Nucl. Mater. 245 (1997) 108.

[6] S.M. Myers, D.M. Follstaedt, F. Besenbacher, J. Bøttiger, J. Appl. Phys. 53 (1982) 8734.

[7] I. Takagi, H. Kariyama, K. Shin, K. Higashi, J. Nucl. Mater. 200 (1993) 223.

[8] I. Takagi, K. Kodama, K. Shin, et al., Fusion Technol. 25 (1994) 137.

[9] J. Völkl, G. Alefeld, in: G. Alefeld, J. Völkl (Eds.), Hydrogen in Metals I, Springer-Verlag, Berlin, Heidelberg, 1978, p.329.

[10] I. Takagi, K. Yoshida, K. Shin, K. Higashi, Nucl. Instr. Meth. Phys. Res. B84 (1994) 393.

[11] M. Akiyoshi, H. Sakamoto, R. Haraguchi, K. Moritani, I. Takagi, H. Moriyama, Nucl. Instr. Meth. Phys. Res. B232 (2005) 173.

[12] D. Dieumegard, D. Dubreuil, Nucl. Instr. Meth. 166 (1979) 431.

[13] J. F. Ziegler, J. P. Biersack, U. Littmark, The Stopping and Range of Ions in Solids, Pergamon, New York, 1985.

[14] I. Takagi, J. Nucl. Sci. Technol. 29 (1992) 947.

[15] S.M. Myers, S.T. Picraux, R.E. Stoltz, J. Appl. Phys. 50 (1979) 5710.

[16] Y. Fukai, The Metal-Hydrogen System, Springer-Verlag, Berlin, Heidelberg, 1993. p.22.

[17] I. Takagi, Y. Ueyama, T. Komura, M. Akiyoshi, T. Sasaki, K. Moritani, H. Moriyama, Fusion Sci. Technol. 60 (2011) 1523.

[18] I. Takagi, H. Fujita, K. Yoshida, K. Shin, K. Higashi, J. Nucl. Mater. 212-215 (1994) 1411.

[19] I. Takagi, N. Matsubara, M. Akiyoshi, T. Sasaki, K. Moritani, H. Moriyama, J. Nucl. Mater. 363-365 (2007) 955.

[20] I. Takagi, S. Watanabe, S. Nagaoka, K. Higashi, Fusion Technol. 41 (2002) 897.

[21] K. Arakawa, R. Imamura, K. Ohota, K. Ono, J. Appl. Phys. 89 (2001) 4752.

[22] K. Arakawa, H. Mori, K. Ono, J. Nucl. Mater. 307-311 (2002) 272.

[23] E. Wakai, Y. Miwa, N. Hashimoto, et al., J. Nucl. Mater. 307-311 (2002) 203.

[24] Y. Dai, X. Jia, S. A. Maloy, J. Nucl. Mater. 343 (2005) 241.

[25] R. Gibala, Trans. Metall. Soc. AIME 238 (1967) 1574.

[26] J.-Y. Lee, J.-L. Lee, Phil. Mag. A 56 (1987) 293.

[27] K. Ono, M. Meshii, Acta Metall. 40 (1992) 1357.

[28] K. Morishita, R. Sugano, B.D. Wirth, et al., Nucl. Instr. Meth. B202 (2003) 76.

Table 1 List of samples.

Sample	$^3He^+$ irradiation				NRA by $^3He^+$	
	Energy (MeV)	Fluence (m^{-2})	*Q* (dpa)	*T* (K)	Energy (MeV)	*T* (K)
A	0.8	1.7×10^{21}	1.2	453	1.7	355-568
B	0.8	1.7×10^{21}	1.2	453	1.7	355-523
C	0.8	2.5×10^{21}	1.7	453	1.7	453
D	1.3	4.1×10^{20}	0.31	370	2.0	370

List of Figure Captions

Fig. 1. Deuterium depth profiles of Fe sample at 453 K before and after irradiation with 0.8 -MeV ^{3}He ions.

Fig. 2. Depth profile of trapped deuterium in Fe sample irradiated with 0.8 -MeV ^{3}He. Distributions of vacancies and ^{3}He ions estimated using the TRIM code are also shown in arbitrary units.

Fig. 3. Depth profile of trapped deuterium in Fe sample irradiated with 1.3 -MeV ^{3}He. Distributions of vacancies and ^{3}He ions are also shown in arbitrary units.

Fig. 4. Temperature dependence of the deuterium concentration in the trap, C_t, and in the solution site, C_s, for sample A. A filled symbol represents the C_t after annealing at 568 K for 1 h.

Fig. 5. Equilibrium constant for partitioning of deuterium between the trap and the solution site in ^{3}He-irradiated Fe.

Fig. 6. Evolution of the trap density with atomic displacement in ^{3}He-irradiated Fe.

Fig. 7. Dependence of the trap site occupancy, C_t/C_0, and the concentration ratio, C_t/C_s, on the solution site occupancy, C_s/hN.

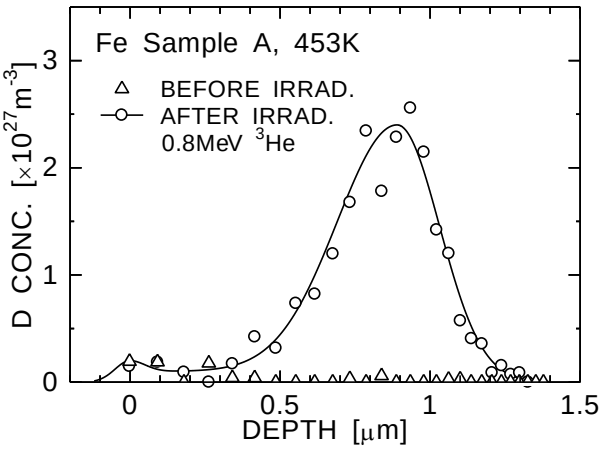

Fig. 1

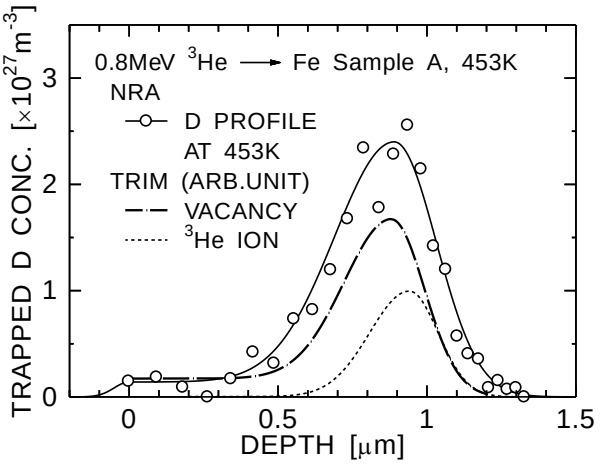

Fig. 2

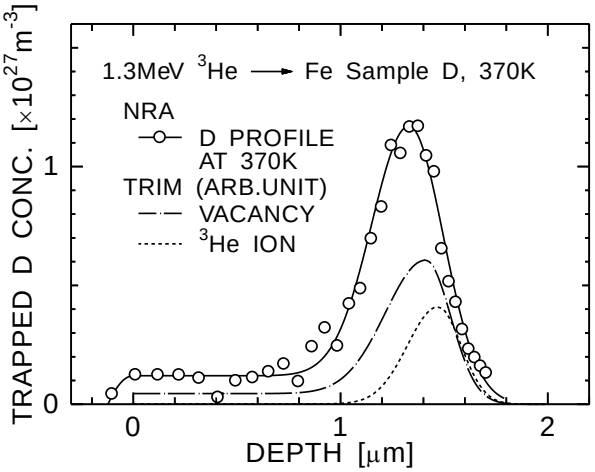

Fig. 3

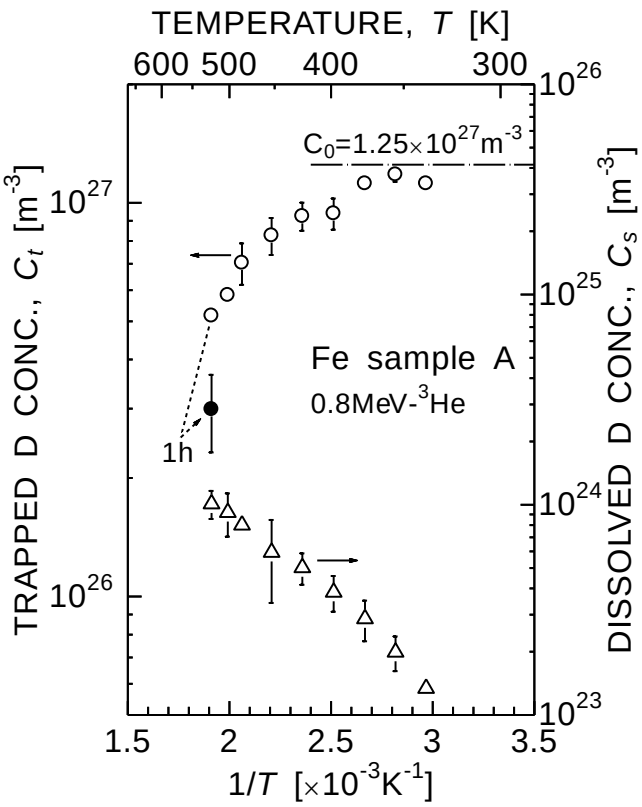
TEMPERATURE, T [K]
600 500 400 300
C0=1.25×10^27 m^-3
Fe sample A
0.8MeV-3He
1h
TRAPPED D CONC., Ct [m^-3]
DISSOLVED D CONC., Cs [m^-3]
10^27
10^26
10^26
10^25
10^24
10^23
1.5 2 2.5 3 3.5
1/T [×10^-3 K^-1]

Fig. 4

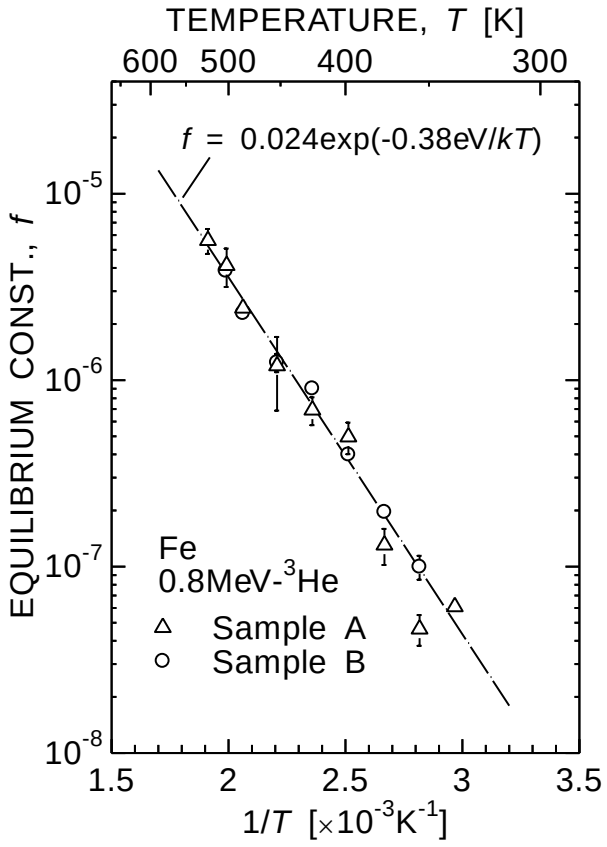
TEMPERATURE, T [K]
600 500 400 300
f = 0.024exp(-0.38eV/kT)
EQUILIBRIUM CONST., f
10^-5
10^-6
10^-7
10^-8
Fe
0.8MeV-3He
Sample A
Sample B
1.5 2 2.5 3 3.5
1/T [×10^-3 K^-1]

Fig. 5

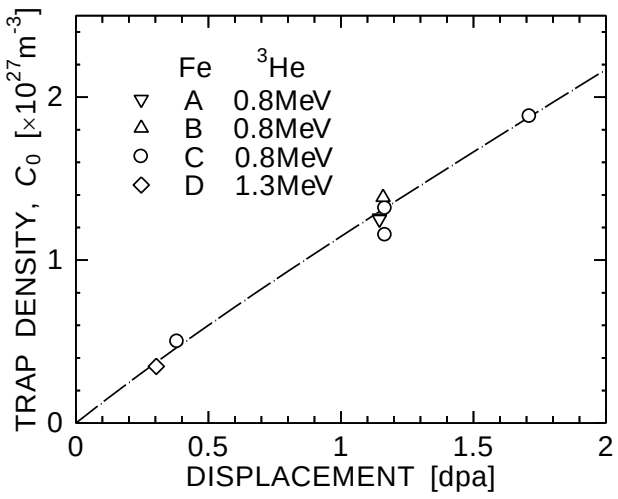
Fe ³He
A 0.8MeV
B 0.8MeV
C 0.8MeV
D 1.3MeV
TRAP DENSITY, C_0 [$\times 10^{27}$m^{-3}]
DISPLACEMENT [dpa]
0
0.5
1
1.5
2

Fig. 6

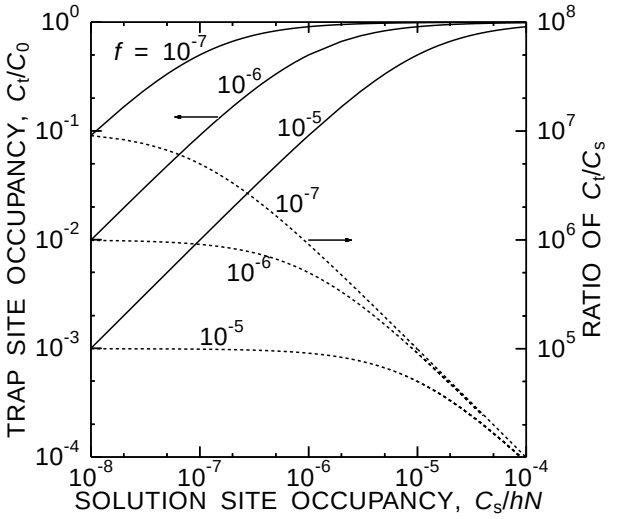
f = 10^{-7}
10^{-6}
10^{-5}
10^{-7}
10^{-6}
10^{-5}
TRAP SITE OCCUPANCY, C_t/C_0
RATIO OF C_t/C_s
SOLUTION SITE OCCUPANCY, C_s/hN

Fig. 7